

Optimal Integration of Electric Vehicles in Smart Grid Energy Flow



Sorin Deleanu, Marilena Stanculescu, Dragos Niculae, Paul Cristian Andrei, Lavinia Bobaru, and Horia Andrei

Abstract This chapter provides an insight into the rapidly growing domain represented by the plug-in electric vehicles (PEV) in connection with the smart grid power system (SGPS) and bi-directional power flow. The chapter starts with an introductory Sect. 1, followed by Sect. 2, containing a review of the main aspects, which define and characterize the interaction between the EVs and the SGPS. The analysis regarding the integration of the EVs into the SGPS under the vehicle to grid (V2G) considered the three main directions: SGPS efficiency improvement, cost-effectiveness, and the reduction in greenhouse gases. After a presentation of the SGPS structure, Sect. 2 includes a brief description of the primary power produced by the wind turbine as well as the one produced by the photovoltaic panels. Both represent input powers to the SGPS, fact which classifies these two elements of SGPS as power sources, although with an intermittent character. Following Sect. 3 dedicated to the charging stations, the chapter continues with Sect. 4 allocated to modeling, simulation, and results. Firstly, this section contains detailed models dedicated to the analysis of battery charging and battery discharging, with applications to individual vehicles and considering the presence of renewable energy sources. The models expanded

S. Deleanu (✉)

SAST, Northern Alberta Institute of Technology, Edmonton, Canada

e-mail: sorind@nait.ca

M. Stanculescu · D. Niculae · P. C. Andrei · L. Bobaru

Department of Electrical Engineering, University Politehnica Bucharest, Bucharest, Romania

e-mail: marilena.stanculescu@upb.ro

D. Niculae

e-mail: dragos.niculae@upb.ro

P. C. Andrei

e-mail: paul.andrei@upb.ro

L. Bobaru

e-mail: lavinia.bobaru@upb.ro

H. Andrei

Doctoral School of Engineering Sciences, University Valahia, Targoviste, Romania

e-mail: hr_andrei@yahoo.com

© The Author(s), under exclusive license to Springer Nature Switzerland AG 2021

N. Mahdavi Tabatabaei and N. Bizon (eds.), *Numerical Methods*

for Energy Applications, Power Systems,

https://doi.org/10.1007/978-3-030-62191-9_22

to multiple vehicles, scenarios, and simulations, including the discussions accompanying the results. In the last Sect. 5, the authors present the conclusions. The chapter concludes with an up to date section of references.

Keywords Electric vehicles · Smart grid power system · Charging stations · Energy flow

Nomenclature

A. Acronyms

<i>PEV</i>	Plug in Electric Vehicle
<i>EV</i>	Electric Vehicle
<i>SGPS</i>	Smart Grid Power System
<i>RES</i>	Renewable Energy Sources
<i>V2G</i>	Vehicle to Grid
<i>PSS</i>	Power System Stabilizer
<i>SOC</i>	State of Charge
<i>SC</i>	Solar Cells
<i>ASC</i>	Area of the Solar Cells
<i>PV</i>	Photovoltaic Panels
<i>EENC</i>	Expected Energy Not Charged
<i>CS</i>	Charging Subsystem
<i>ESS</i>	Energy Storage System
<i>EPDS</i>	Electric Power Distribution Subsystem
<i>AES</i>	Auxiliary Energy Subsystem

B. Symbols/Parameters

P	Power
P_{rated}	Rated power
P_{wind}	Power delivered by the wind turbine
ε	Albert Betz constant
ρ	Air density
A	Area cleared by the wind turbine
V	Speed
$v_{rated,w}$	Rated speed of the wind turbine
$v_{min,w}$	Minimum wind speed to allow the wind energy production
$v_{max,w}$	Maximum wind speed allowed for wind turbine safe operation
$P_{SC}(t)$	Output power of the solar cells
A_{SC}	Area of the solar cells
η_{SC}	Efficiency of the solar cells
$P_{PV}(t)$	Output power of the photovoltaic panels
A_{PV}	Area of the photovoltaic panels

η_{PV}	Efficiency of the photovoltaic panels
$\mu(t)$	Solar insolation
$V_{int,rec}$	Rectified (DC) voltage
V_R	Voltage across the equivalent resistor of the charger
V_{cap}	Voltage across the equivalent capacitor of the battery
V_{out}	Voltage at the output of the charger operating as rectifier
i_1	Current at the input to the charger
i_2	Current at the output of the charger
η_C	Efficiency of the charging station operating as rectifier (charging)
R	Resistor
C	Capacitor
V_{in}, V_{out}	Input, respectively output voltage
i_{in}, i_{out}	Input, respectively output current
P_{in}, P_{out}	Input, respectively output power
T_C	Charging time constant
T_{max}	Duration necessary for battery to fully charge from zero power
P_{max}	Maximum power at the battery
t_1	Initial moment of the charging process
$P(t_1)$	Battery power level at the beginning of the charging
$P(t'_1)$	Battery power level at the beginning of the discharging
P_{BPEV}	Instantaneous power level of plug in electric vehicle battery
$P_{BPEV,max}$	Maximum power level of plug in electric vehicle battery
$P_{BPEV,dem}$	Instantaneous power demand of plug in electric vehicle battery
α, α_i	Charging constant of the plug in electric vehicle battery
$P_{BPEV,max}$	Maximum power level of plug in electric vehicle battery
$P_{BPEV,dem}$	Instantaneous power demand of plug in electric vehicle battery
E_{BPEV}	Energy necessary for the plug in electric battery to fully charge
$\Delta t_i, i = 1 \dots 4$	Time interval
ΔT_{Fault}	Duration of the fault interval faced by the PEV battery during charging
$\gamma_{dis}, \gamma_{disk}$	Discharging constant of the plug in electric vehicle battery
n_{PEV}	Number of electrical vehicles in charging/discharging process
N_{st}	Number of charging stations
$P_{BPEV,inj}$	Power injected into the supply by the batteries of the PEV fleet
η_i	Efficiency of the charging station converter operating as inverter (V2G)
$P_{BPEV,dis}$	Power level of the plug in electric vehicle battery following discharging
P_{Lim}	Lower level specified for the plug in electric vehicle battery power
$P_{BPEV,net}$	Net power exchanged between the supply by the batteries of the PEV fleet
$P_{Renewables}$	Power injected into the SGPS by RES at the point of common coupling with the charging station
G_{Power}	Power gain at the connection point between the parking lot and power supply

G_{En} Energy gain at the connection point between the parking lot and power supply

1 Introduction

All the EV utilizing rotational motors for producing the tractive effort, display similar configurations of their power systems responsible for torque production and its conversion into the traction force applied at the wheel. Such systems consist of a primary energy source, converter(s), and rotational electric motors, eventually a gearbox and traction wheels. In the latest applications, one can observe a trend to integrate the assembly motor–traction wheel in a subcomponent eliminating the need for the differential gearbox. The autonomous electric vehicles, presented in the first section of this chapter, operate based on a primary source of energy, including a system of rechargeable batteries. Their connection to the power grid generally occurs during their parking time. Purely electric vehicles rely on batteries exclusively, whereas plug-in hybrid vehicles (PHEV) contain a fossil fuel-based primary energy source as well.

The implementation in the last decade of newly restrictive norms regarding the pollution reduction and climate change mitigation, targeting agglomerated metropolises from several developed countries, determined a significant increase in the percentage of EV from the total number of vehicles on the road.

Consequently, the autonomous EV fleet became a direct and essential player regarding the processes of energy conversion, transfer and distribution, working within SGPS which includes renewable energy sources (RES) as well. Ignoring the interaction between the electric vehicles and the SGPS became practically impossible, given the bi-directional character of the energy transfer. The electric energy flows from the grid to the vehicles during the battery recharging process, and conversely from the vehicles to the grid, mostly during the hours of highly local power demand. In the last case the electric vehicles, having their batteries charged enough, act as generators whereas the grid absorbs the electrical energy.

Section 2 of this chapter provides details regarding the bi-directional transfer of electric energy. The inherent involvement of the power electronic converters in the process of the electric energy transmission, no matter their location, inside the grid or belonging to the electric vehicles, may result in the generation of current harmonics. These harmonics can circulate through the power system, influencing the operation of its components through the production of further losses, heating, and determining an overall efficiency decrease. Some components of the SGPS may become victims of this phenomenon, which overall affects the power quality of the system. This section includes details regarding the classification of components interacting within an SGPS. It delivers insight regarding the ancillary services provided by the EVs, and their implications in terms of battery lifespan. There is a presentation of standards and

norms concerning both the EVs and SGPS reflecting the complexity of the interaction level, including economical aspect as well as energy management.

Section 3 focuses on the charger's classification and performances, as well as on solutions regarding the charging stations and the correlation between the driving habits and the status of the battery.

The main objective of Sect. 4 is the analysis of the optimal integration of electric vehicles into the smart grid. Such a problem is very complex presenting significant considerations related to the distribution of the parking areas and their types of charging stations, the locations assigned to the power regulators and power system stabilizers (PSS) and the performances of such devices, the types of vehicles in the system, the demand in recharging power at the moment or conversely the power delivered by the vehicles and consumed by the grid, the minimization of the losses and costs required by the bi-directional energy transfer through the ongoing efficiency maximization. The case of study and the adjacent simulations performed utilizing the well-known MATLAB program answers to the requirements highlighted above.

The final section contains the conclusions of this work, and the chapter ends with numerous and consistent list of up-to-date bibliographical references.

2 Electric Vehicles, Smart Grid Power System and Bi-directional Energy Flow

The understanding of EV integration into SGPS, nowadays, requires familiarity with the vehicle to grid (V2G) concept, firstly introduced by Kempton [1], in 1997, which proposes the utilization of EVs as sources for the SGPS. An SGPS includes RES, storage units, and eventually, classical energy sources, based on fossil fuel (see Fig. 1) [2]. The structure of an SGPS, according to the National Institute of Standards and Technology (US) contains the following divisions [3]:

- *Generation*
- *Transmission*
- *Distribution*
- *Service Providers*
- *Consumers (customers)*
- *Energy Market*
- *Operations*

At this point, there is no direct reference to the terms such as V2G, aggregator, whereas the customers are not candidates for energy storage, suitable for involvement in V2G action.

The storage units can include or be exclusively EVs, whereas small scale applications may not contain classical sources. Continuously increasing EV fleet around the globe comes with the drawback of the massive charging demand, which strongly impacts the power grid components such as generators, transformers, distribution

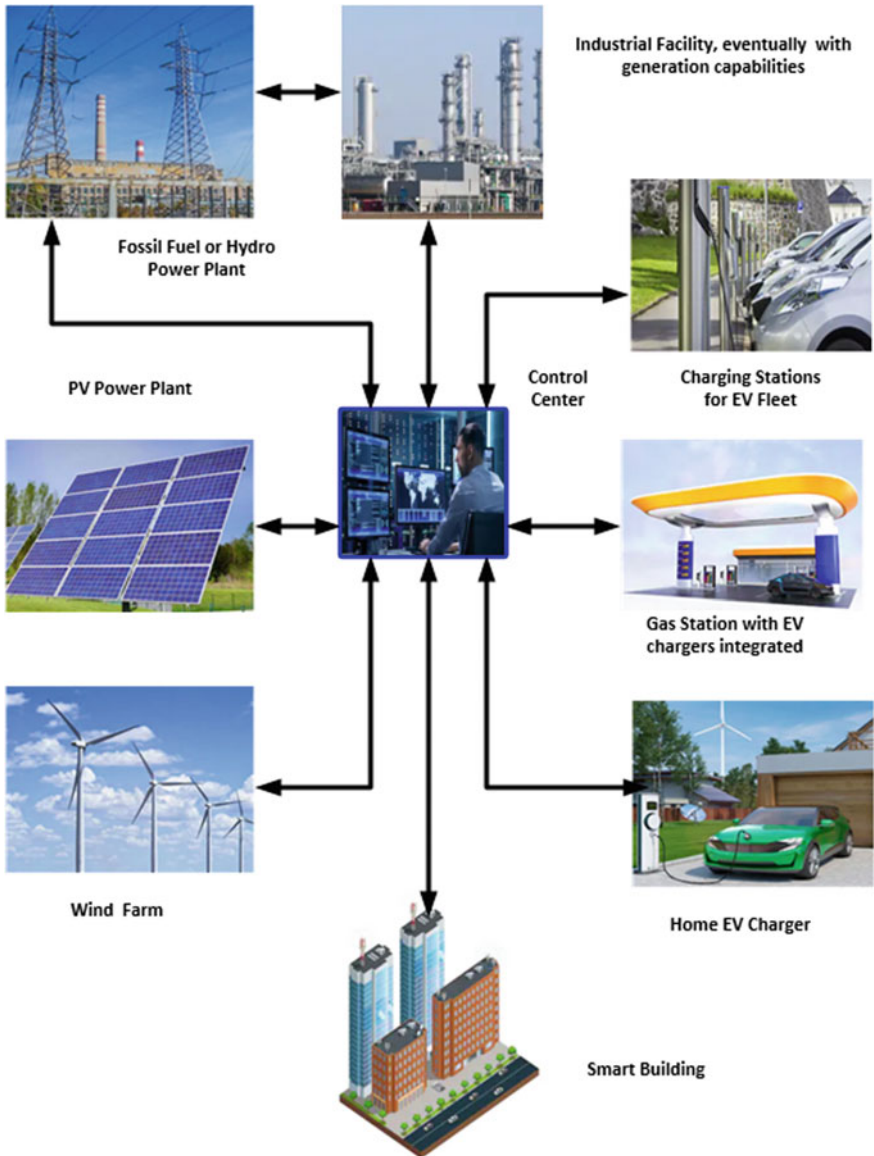


Fig. 1 One smart grid configuration

cables. Interconnection between the local power system, RES and charging stations may represent the critical solution for the mitigation of the drawbacks mentioned above. Moreover, it can lead to a decrease in the amount of greenhouse gases released into the atmosphere and in the EVs charging cost, as well [2–6].

Assuming substantial scale participation of RES, one must account for their significant dependence on weather conditions, generally resulting in either surplus or deficit of delivered energy and, consequently, hardship concerning dispatching it. Participation of the EVs considered working under the V2G technology, can significantly improve the overall SGPS stability by smoothing the power and voltage profiles versus the time, whereas playing the character of storage system for the energy delivered by RES or being an intelligent consumer through an intelligently planned and coordinated EVs battery charging process.

The interaction between the SGPS, RES, and EVs follows three distinct directions [2]:

- *SGPS efficiency improvement*, utilizing the EVs batteries as energy buffers; EVs charging takes place when the RES energy is in excess to the grid absorption availability, whereas EVs batteries deliver electric power to the supply when an SGPS experiences power deficit.
- *Cost-effectiveness*, results in preoccupation for minimization of electricity generation, charging and operation and maximization of the provider's profit.
- *Reduction in greenhouse gas emissions*.

The main difference between EVs and the vehicles utilizing engines with internal combustion resides in the nature of the engine itself. The autonomous EVs primary's source is either a power generator (e.g., diesel-electric or gas-turbine based locomotives, in which cases the prime mover of the generator is an internal combustion engine) or a storage system existing on-board, mostly batteries. Most of the current EV employs the last type of source. There are two main categories of EVs [2]:

Battery Electric Vehicles: The power plant of EVs compatible to V2G technology consists of a rechargeable battery storage system, an electric motor (permanent magnet synchronous, induction or switched reluctance), and a four-quadrant fully-controlled power converter (i.e. composed from two fully-controlled rectifiers, the one 's positive output rail being the negative for the other, and conversely).

Plug-in Hybrid Electric Vehicles: Relying on a battery storage system and a fuel tank as well, the power plant contains two motors for a combined propulsion system, one electric and another one with internal combustion, although they don't operate simultaneously. With the vehicle in the charge depleting mode, the electric motor drives the vehicle, getting its input electric power from the batteries, until the battery reaches the lowest charge threshold. At this point, the control system switches the traction responsibility to the internal combustion motor, which carries the extra responsibility of charging the battery system to the highest state of charge threshold limit, giving the possibility to the controller to switch back to the electric motor. Such an operation is called parallel-hybrid [2]. Lithium-ion batteries, the main elements fulfilling the energy storage function of the duality SGPS–EVs, possess a high density of energy, long life span, and minimal environmental impact. However, they require special attention from the control systems apropos the charging/discharging process, improper voltage/current variations resulting in battery damage. RES is the main component of an SGPS, and the most known types are the wind energy and solar energy, yet both are highly weather dependent.

2.1 Wind Energy Based RES

The appropriate placement of wind farms improves the efficiency of energy conversion from wind to electrical and increases the output of electrical energy. The wind speed determines the amount and the quality of wind energy, and there are several proposed methods for the evaluation of the wind speed and power summarized in [2], using the approach of Peterson and Hennessey:

$$(v/v_r) = (h/h_r)^a \quad (1)$$

In (1), v is the wind speed at height h , whereas the wind speed v_r is known for the reference height h_r , and the coefficient a belongs to the interval 0.1–0.4.

The amount of wind energy with the potential of conversion into electrical energy, for the wind speed (1), strongly depends on atmospheric conditions such as wind speed and air density [2]:

$$P = 0.5\varepsilon\rho Av^3 \quad (2)$$

The coefficient α designates the constant of Albert Betz, ρ (kg/m^3) is the air density, A (m^2) is the cleared area by the wind turbine, whereas v (m/s) is the wind speed. The employment of several available expressions may correlate the wind power to the wind generator rated value, as in (3a–3c) [2]:

$$P_{wind} = 0, \text{ if } v < v_{\min,w} \text{ or } v > v_{\max,w} \quad (3a)$$

$$P_{wind} = P_{rated} \left(\frac{v^3 - v_{\min,w}^3}{v_{rated,w}^3 - v_{\min,w}^3} \right), \text{ if } v_{\min,w} < v < v_{rated,w} \quad (3b)$$

$$P_{wind} = P_{rated}, \text{ if } v_{rated,w} < v < v_{\max,w} \quad (3c)$$

In (3a–3c), v is the wind speed, $v_{\min,w}$ represents the minimum speed of the wind for which the wind turbine is capable to produce electric power, $v_{\max,w}$ the maximum wind speed at the wind turbine can safely operate, P_{wind} is the wind power, P_{rated} is the rated power of the wind generator, $v_{rated,w}$ is the rated wind speed.

2.2 Solar Energy Based RES

Representing the primary energy for the other principal RES, solar energy conversion into electrical energy occurs directly through photovoltaic panels (PV) or indirectly from solar to thermal, then into electrical. In the second case, specialized installations, utilizing mirrors and lenses to focus sunlight, target water tanks placed on tall

reinforced mechanical structures. By concentrating the solar power on the radiation absorbent surface of the water tank, the water is transformed into steam, reaching the appropriate parameters for driving a steam turbine as a prime mover for a generator.

PVs are constructed with solar cells (SC), and display an efficiency which slightly varies with the temperature, practically decreasing with 0.2–0.5% for every 10 °C increase [2].

In addition to the SC efficiency η_{SC} , the electrical power output P_{SC} for an aggregated area of SC depends on the surface of its area A_{SC} (m²), respectively by the solar irradiation s (W/m²) (4), which is practically the only variable parameter [2]:

$$P_{SC}(s) = \eta_{SC}sA_{SC} \quad (4)$$

The output electric power of a PV solar panel depends on its area A_{PV} (m²), its efficiency η_{PV} , respectively on its solar insolation $\mu(t)$ [2] (5):

$$P_{PV}(t) = \eta_{PV}\mu(t)A_{PV} \quad (5)$$

Modeling of wind and solar energy to improve the quality of feasibility studies regarding this RES placement, integration, and utilization, required linear, nonlinear and artificial intelligence to predict the wind and solar energy in specific locations [2–6]. The integration of the EVs into the SGPS occurs under the surveillance of a third party, called *aggregator*. Even though the main feature of the V2G technology is the bi-directional power flow between EVs and SGPS, meaning that the EVs are electrical energy buffers utilized to compensate for the RES intermittency and weather determined irregularities in energy delivery, shaving the peaks and leveling the load “seen” by SGPS, there are ancillary services requested from EVs [4]:

- *Power regulation*, which means the frequency regulation, matching the energy generation with the load demand.
- *Warm or Spinning reserve*, representing the short term (less than 10 min) fast response additional generation capacity to act in case of outage rapidly.
- *Reactive power compensation*, utilizing the reactive power delivered by the capacitor present in the DC link of the fully controlled four-quadrant drive.

The owners of the EVs integrated into the SGPS must have the acknowledgment for the battery lifespan reduction due to a continuously variable charging-discharging cycle, in the form of proper compensation. The integration of EVs into SGPS has a multitude of impacts on the SGPS. Many authors agree [3, 7–28] on the EVs presence impacting the operation of the *distribution systems, system’s equipment, load capacity, power quality, economy, social life and nevertheless, the environment*.

The impact of the EVs penetration on distribution system reliability, presented in [11] assumes different levels of EVs penetration in the SGPS, in the presence of V2G technology.

The factor named Expected Energy Not Charged (EENC), measures the reliability of the system from the viewpoint of EVs integrated with the SGPS, and requires the addition of the energy loss during charging to the energy loss because of unscheduled

V2G. The authors signal better reliability of the SGPS with distributed generation in the presence of EVs.

For example, whereas applying a stochastic model of the EVs energy needs and starting from a load flow study, Anastasiadis et al. [12] concluded that the voltage levels at the nodes where EVs are present fluctuate in a prescribed range, with the application of a smart charging strategy within V2G.

In [13], there is an assessment of the transformers aging due to the penetration of the EVs, using a stochastic method modeling of the transformer's life consumption. Here, the load model applied to EVs, originated from an analytical solution used for predicting a cluster of EV chargers. The authors disclosed results that show a severe 44.1 h of the loss of life for every 24 h of operation, during the summer and with an EV penetration of 50%, whereas a penetration of 10% or less does not decrease transformer's life. However, the transformer's life loss depends on the load level and its temperature at each moment. High EVs penetration level unfavorably impacts the power transformer lifespan, following a study involving the calculation and analysis of the dielectric oil deterioration [14], showing consistency with [13].

Furthermore, there are economic and social aspects of the EVs integration debated in [15–18]. For example, in [15], a study targeting EV users in Germany concluded the presence of substantial concern, especially for high mileage drivers, regarding the range decreasing and loss of availability to drive the vehicle during the long hours of connection to the SGPS. The authors found that a promising remuneration for participating in V2G couldn't mitigate the concern. The costs regarding infrastructure, electricity sale by the vehicles and the battery degradation appeared the most important factors regarding the feasibility of the V2G implementation, to obtain income from the energy supplied to a commercial building [16].

The cost of EVs operation, together with the rules governing the energy market, have an influence on the participation of the EVs into a centralized V2G system [17]. This study indicates a profitable grid (here called virtual power plant), a system operator with fulfilled services and EVs being on the money-losing side. Cost elements face the revenue element in a study focused on determining the critical economic factors of the V2G technology implementation [18]. The factors considered in the *cost* side are the battery lifespan reduction and replacement, the V2G capable power electronic converters (i.e., many vehicles need retrofitting and installation of such converters), the infrastructure of charging stations, nonresidential and residential, the hardware equipment and its specialized software required for communication and the aggregator as network manager. An aggregator has proven to be costly (i.e., may necessitate up to 50% revenue for covering its expenses and obtaining some profit) as well, directly associated to its main tasks of EVs control, networking services, contract management with EV owners, activity on energy markets and availability for unexpected services. The elements offering potential *revenues* are the pool of aggregated EVs, daily number plug-in hours, the power availability (kW) for transfer from EV fleet to SGPS, the level of available energy (kWh) for specific conditions of demand and price.

One can perceive the EVs as receptive loads, whereas integrated into SGPS provide ancillary services and reserve power under proper scheduling from the aggregator, responding to the energy and reserve requirements. Such scheduling positively influences the load profile by flattening it through charging/discharging time allocation [19]. However, in [20] the authors extrapolate the aggregator's role from the business controller into the highly bonded interface between the EVs and SGPS, meant to implement and monitor the EVs function of providing ancillary services.

The EVs integration into SGPS displays not only potential benefits but very many challenges, as well. The overall interaction between the EVS and SGPS under the V2G technology requires proper scheduling mechanisms, to address the challenges, fact which turns the need for *optimal scheduling* into a priority [21–28]. There are many objective functions possible to define and undertaken by scientists, very much trying to answer to individual objectives, associated with real applications. In [21, 22], the authors raise the problem of dimensioning and placement for a distributed generation system, built with small power units, issues followed by the bi-directional power flow investigation. In [21], the debated problem has the first stage, while the clear objectives are the power loss minimization and voltage regulation. In the second stage, the objective function represents the amount of RES, including the EVs, followed by the optimization of the rate of charge. Consequently, to the application of a genetic algorithm to a system with 30 buses, the authors found the optimum power ratings of the distributed generators as 450 kW and 550 kW, respectively. Moreover, the minimization of the power loss indicated the placement for EV chargers.

In [22], there is an inclusion of RES (i.e., 10 wind turbines and 117 photovoltaic panels) in a distributed generation system, which becomes capable of sophisticated control of the EV batteries charging and discharging, minimizing the power loss and regulating the voltage as well. Intelligent scheduling considering the EV batteries charging and discharging process in conditions of energy price constrains, initiated a study focused on maximum profit demanded by the EV owners through a proper charging/discharging time rate [23].

Although the applications from [21–23] addressed common parking lot facilities for EVs, in [24], the authors proposed a study aiming to solve the optimal control of smart buildings with EV charging capabilities, with the objectives of minimizing the power loss and maximizing the comfort for customers. The optimizing technique is a combination between the particle swarm algorithm and the multi-agent technology. Then, a carried-out simulation employed an extended system with 500 wind generators and 400 photovoltaic panels in a time frame of 24 h. Simulation has proven the possibility to acquire a high level of comfort, even during periods with energy deficit recorded for isolated buildings.

A solution to the energy concern in a small-scale system, including aggregated EVs and working within V2G technology, exists in the form of a robust optimization model based on linear programming [25]. In such a model, the authors suggest an assessment of the V2G impact on the system's energy management. In the case of EVs presence in large numbers, there is a demand for coordination between the EV

fleets given their role as renewable sources as well as storage units within the bi-directional power flow under V2G technology. Simulation results from [26], recommend an optimal scheduling power flow inside the SGPS, whereas the EV fleets are stationary. Frequency regulation is one of the primary ancillary services potentially provided by EVs, together with their role as load leveling and on-waiting (i.e., instant readiness) reserves. However, SGPS frequency regulation may result in Li-ion battery degradation [27]. The mitigation of such a drawback became possible with the application of a smart algorithm pointing to the maximization of the battery life span. More precisely, the battery of an EV connected to the grid can deliver energy only if it is fading, evaluated through a proper forecast model about reaching its lowest acceptable level. If did, the respective battery can only receive electrical energy from the supply.

Frequency regulation with the participation of EVs is the main topic in [28] as well. This time the deciding factor being the battery state-of-charge (SOC), assessed by calculating the owner's driving demand with a specially designated module. Financial aspects of the EVs integration into SGPS are essential for the EV owners, willing to allow their cars to provide auxiliary services to the grid, as well as a stand-by reserve to the grid. However, two studies from 2016, [29, 30] recognized that the revenues from aggregators are by far insufficient to make the V2G technology attractive (i.e., from 20 times less to 27,500 less) under the present-day market and regulations in place. The EV battery in V2G is facing a permanent cycle of charging-discharging if stays connected to the power system, and consequently, its life span shortens, and there is no mechanism in place to encourage the owners to participate in V2G other than potential government subsidies. Moreover, the relatively reduced number of EVs didn't assure the stand by (aka fast) firm reserve for more than a few hours. The most optimistic prediction regarding V2G cost-effectiveness mentions the year 2030. Consequently, one must address the amount of annual profit to satisfy all, the aggregator and the EVs owners into a joint venture towards V2G. The integration of EVs into SGPS, under several business models, resulting in contracts between the SGPS owners and the aggregators, must consider the EVs battery charging stations, containing data centers, as essential participants in SGPS regulations [3]. The National Institute for Standards and Technology (NIST, US) decides the standardization direction for security and reliability on the smart grid. For example, the guidelines for SGPS cybersecurity have its place into NISTIR 7628. To be feasible, an actual SGPS must fulfill many conditions, such as [3]:

- (1) *Participation of RES with possibility of increasing it*
- (2) *High power quality*
- (3) *High resilience to disruptive events*
- (4) *Increased operational efficiency of its components and overall*
- (5) *Robustness to disturbances and self-healing*
- (6) *Capability to accommodate drive storage units*
- (7) *High level of cyber security and capability of ongoing improving it*
- (8) *Flexibility in terms of consumer's selections*
- (9) *Smart revenue metering*

- (10) *Reduced amount of greenhouse gases by encouraging the progressively larger participation of EVs, actively working under V2G technology: bi-directional electric power flow.*

Subsequently, understanding the actual standards applicable to EV and SGPS becomes vital. Whereas Table 1 presents the standards for EVs elaborated by the Society of Automation Engineers (SAEJ), in the Table 2 (IEC), respectively Table 3 (IEEE) one can find the most critical standards in place, referring SGPS, from all over

Table 1 Most important SAEJ standards for EV, US [3]

SAEJ standard	Domain
1772	Defines the functions of the of the vehicle supply equipment as: coupler, rectification and voltage regulation
2293	Addresses the EV requirements and the off-board equipment used for EV charging
2836	Communication requirements for integrating the vehicle in a V2G technology, specifically to assure the existence of the functions of energy transfer and or energy storage
2847	Communication between the EV and the fast, high power DC off-board charger
2894	Off-board charging practices

Table 2 Most important IEC standards for SGPS [3]

IEC standard	Domain
61000-4-30	Power quality
618500	Communications
14908-3	Power line communication
618500-7-420	Communications including reference to microgrids
61968-9	Advanced/Automated metering
62351	Protection of smart grid
61970	Communication and metering data exchange
62056	Communication and metering data exchange
61968	Communication in distribution
11518-2	Communication between smart grid networks
TC57-WG13	Cybersecurity and reliability in smart grids
60870	Inter-control center protocol
62056	Metering, load control an tariff
14543	Home electronic system architecture
61400-25	Operation of the wind power plants

Table 3 Most important IEEE standards for SGPS [3]

IEEE standard	Domain
P2030	Interoperability requirements
C37.118.1-2011	Security
1588	Smart grid interoperability and control
2030-2011	Smart grid interoperability and control, communication infrastructure
1377	Advanced/Automated metering
1547.4	Micro grid
1547.6	Distributed networks
1451	Smart sensors
145.1	Wireless sensor network
1646	M2M communication
802.16	M2M communication
61499	Control in smart grid
ZigBee 802.15.4b (wireless, V2G, dedicated for installation at client)	Communication frequency: 2.4 GHz (anywhere in the world) Distance covered: 10–100 m
Wi-Fi 802.11 g (wireless, V2G)	Communication frequency: 5.85–5.95 GHz Distance covered: 0.5–1 km
Bluetooth 802.15.1a (wireless, V2G)	Communication frequency: 2.4 GHz Distance covered: 1–100 m
WiMAX 802.16 (wireless, V2G)	Metropolitan area network Frequency: 2–6 GHz Distance covered: 2–5 km
6LoWPAN 802.15.4	Communication
WRAN 802.22	Communication
901	Power line communication
802.3ah	Optic fiber communication
802.3	Ethernet
1701	Metering devices
1702	Metering devices

the world [3], and their development responded in essence to six directions: operation, power quality, metering, communication, protection & control, and cybersecurity.

3 Requirements for PEV Charging Stations and Smart Grid Power System

A station used for charging EVs is a system consisting on four main subsystems (see Fig. 2), namely:

- Charging subsystem (CS)
- Energy Storage System (ESS)
- Electric Power Distribution subsystem (EPDS)
- Auxiliary Energy subsystem (AES)

The duty cycle of a charging station for EVs can have a duration of 24 h. Such a duty cycle strongly depends on the user’s daily schedules, with the highest demand recorded during the daytime because of the heavy traffic. Consequently, the modeling of the EV charging process considers three periods:

- *Model 1*, called of high energy consumption, with a duration denoted with T_r between 7.00 am and 3.00 pm
- *Model 2*, called of medium energy consumption, with a duration T_m , between 3.00 pm and 11.00 pm
- *Model 3*, called of low energy consumption, with a duration T_s , between 11.00 pm and 7.00 am next day

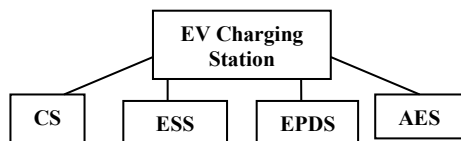
Using the previous notations becomes obvious that $T_r + T_m + T_s = 24 h$. The demand for efficiency in conditions of lowest possible electrical energy market price encouraged the EVs users to proceed for battery charging only during night time, between 11.00 pm and 7.00 am. There are several charging possibilities available for EV users, whereas the Standard IEC 61851 defines four charging modes [3]:

Charging mode 1. In this mode, the charging location represents a standard outlet, generally used for domestic appliances at 120 or 230 V AC.

Whereas the EV is in *charging mode 2*, the electrical connection of the EV battery to an AC outlet for general-purpose requires a standard cable that incorporates a control device, capable of interacting with the outlet. Such a control device keeps the battery charging current below its maximum threshold, monitoring the outlet quality as well, more precisely the voltage drop level as a good indicator for an over temperature condition. Automatically, the battery charger turns-off in case of a fault.

In the *charging mode, 3* the outlet comes connected to a specially designated circuit; this fact assures the real-time communication between the EV and the electric installation. There is a need for the installation of a specialized electronic device at the location.

Fig. 2 The structure of a station used for charging EV



Charging Mode 4 refers to the fast charge using a DC outlet, utilizing an external charger which includes the charging cable as well. The DC charger delivers the charging voltage itself. Characteristics of such a charging type are the elevated values for the voltage and current. Whereas the DC charging is in place, the connection cable doesn't separate from the charger itself and, consequently doesn't exist any connection to the battery terminals. One can find this type of outlet only on the fast charging terminals. Such an assembly must comply with the world standard CHAdeMO.

The AC charging of type E matches the domestic outlets becoming suitable for charging modes 1 and 2. The so-called plugs of type 1 or type 2 have a clear designation for EVs and belong to the charging stations or the domestic chargers such as Walbox. The domestic or "at home" charging comprises 95% of the total EV battery charging. For single-family homes, the whole process becomes quite simple and relatively easy to monitor. However, not every EV user lives in such a home, a fact which complicates the charging issue.

Moreover, for certain EV brands, the Walbox Mode 3 is a must, as their connection to the standard outlet is not possible, excluding the charging Mode 1 as an option. The Walbox, operating in charging Mode 3, comes highly recommended by its security features, yet financial reasons make many users reluctant to it. Several hours of charging, absorbing 8–10 A of current can potentially overheat the electric cables existing on and involved in the process. Consequently, the whole charging process requires careful monitoring and control. Walbox Mode 3 presents the advantage of the highly safe operation, practically eliminating any electric hazard and providing elevated protection to people and livelihood. For such a solution, the internal micro-processor can permanently control the voltage, current, the charge duration, and its cost, data that becomes accessible to users due to the communication with the EV.

The regular charging outlets from public spaces assure 1–3 h of charging, depending on their power rating and the type of EV as well. Furthermore, the DC fast charging outlets impress the direct current into the batteries, through their rectifiers. The DC charger communicates the same essential information (current, voltage, power, and cost) to the EV through the charging cable.

One classifies the DC outlets as intelligent due to their ability to communicate directly with the EV, delivering data regarding the energy consumed for charging, optimally, and safely. First-generation EV batteries allow the recharging to 80% state of charge from a DC charger in about 20–30 min. Nowadays, the lithium-ion technology made possible manufacturing new batteries with a reduced charging time of 5–15 min to the same 80% state of charge. A typical DC charger can deliver a voltage of 400–500 V, a current of 100–250 A, for a total power of approx. 50 kW. Battery replacement gains terrain at the level of small EV, after proven effective for electric buses used for public transportation. The replacement process takes place in about 3 min (i.e., duration similar to the filling of a full tank) inside of special fully automated dedicated stations. According to SAEJ1772, each type of chargers has three levels, whereas fulfilling the recommended following specifications [3]:

- The AC type charger, Level 1 has single phase voltage, rated at 120 V, current ratings of 12 A or 16 A and consequently the power ratings of 1.4 kW, respectively 1.9 kW. The charging time assigned for the EV is 17 h and for PHEV 7 h.
- The AC type charger, Level 2 has either single phase or three-phase voltage rated at 240 V, a current rating of 80 A, and consequently the power rating of 19.2 kW. The charging time assigned for the EV is 7 h and for PHEV 3 h.
- The AC charger, Level 3 must assure more than 20 kW, without specifying any other characteristics for the present day.
- The DC type charger Level 1 comes with a voltage rating between 200 and 500 V, a current rating less than 80 A, a power rated at 40 kW, a three phase supply connected to the input of the rectifier. The charging time assigned for the EV is 72 min and for PHEV 22 min.
- The DC type charger Level 2 comes with a voltage rating between 200 and 500 V, a current rating less than 200 A, a power rated at 100 kW, a three-phase supply connected to the input of the rectifier. The charging time assigned for the EV is 20 min and for PHEV 10 min.
- The DC type charger Level 3 comes with a voltage rating between 200 and 600 V, a current rating less than 400 A, and a power rated at 240 kW. There are no other specifications for the present time.

Wireless charging requires the presence of two coils. The first one, called the emitter, installed in a box fixed at the ground level and connected to a power supply, produces a magnetic field. The magnetic coupling between the emitter and second coil called receiver placed below the EV allows the magnetic field to induce a voltage across the second coil. The output of the receiver which is directly connected to the input of a rectifier, converts the induced voltage into DC voltage. Furthermore, a filter flattens the voltage shape, which is then applied to the battery terminals, charging it. High losses and low efficiency of about 20%, maintain this charging mode at the level of work in progress, necessitating future research work.

Presently the EV user especially counts on public charging stations, whereas most of the owners depend on home chargers, fast-charging stations or battery replacement stations. Nowadays, there are not enough fast-charging stations nor battery replacement stations: the public charging infrastructure satisfies only 75% of the “100 km/day” EV users. This lack of enough fast charging and or replacement facilities, forces the EV users towards home charging solutions, triggering a significant impact on the energy market. Such a standpoint makes the charging stations to look like completion to home charging outlets. However, current limitation makes the fast charging impossible at home level.

For home charging, one can count for maximum 1/3 of battery charging capacity in three hours; if this is not enough, then highly demanded public fast-charging stations can bring the EV batteries to full charging state in less than 1 h. Although, the large-scale deployment of solar cells, integrated into SGPS under continuous development, may result in the opportunity to provide homes with solar panels enhancing performances of the home chargers. The power and energy densities are the two critical

factors concerning the battery fabrication technologies which face rapid development. One can expect an increase in these two factors predicting an upturn in the EV autonomy, as well.

The integrated power stations represent a new concept, and the construction of such a station must fulfill specific rules, for risk mitigation. Integrated charging stations may be candidates for “safe distance” like requirements, presently applied to infrastructure adjacent to gas stations.

In one suggestive example, one affirms that the safe distance between the charging equipment and the electric power station must be at least 18 m. Moreover, the electrodes from inside the lithium-ion batteries according to their fabrication material belong either to class C (i.e., solid combustible) or class D. In this way the battery represents a synthesis of different materials, possibly assessed as depletion of class C materials.

In another example, one aims the safe distance between the supplied equipment and the warehousing area for batteries: such a distance should be more than 15 m. Following numerous standards and experiences, one can choose the appropriate placement of the charging stations for EVs, mitigating the risks associated with technologies of operation when integrating the chargers into gas stations. A safe distance of 18 m between the gasoline tank and charger’s equipment allows the addition of chargers to the gas station, as shown in Fig. 3.

There are two solutions regarding battery charging management, suitable for *integrated charging stations*:

- (1) The first solution requires the battery charging to take place inside the charging stations, with the following advantages and drawbacks:
 - (1a) one can replace the fading batteries at the right time; there can be an improvement in the EV battery utilization

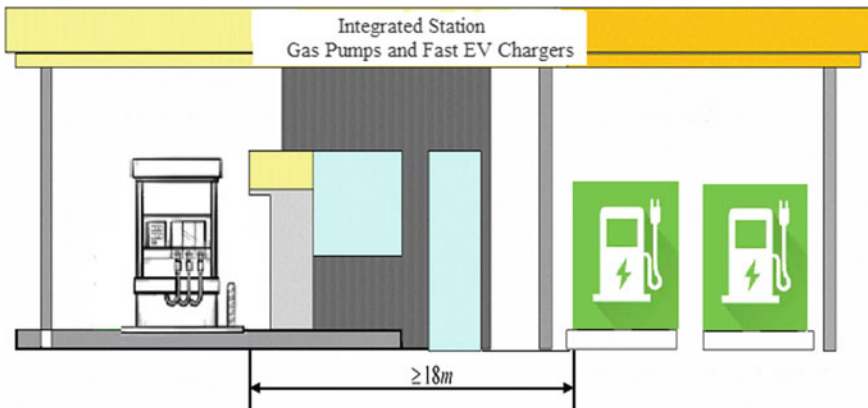


Fig. 3 Gasoline station with integrated chargers for EVs

- (1b) integrated charging stations demand a more performant energy distribution capability, to assure enough energy for battery charging
- (1c) more electric equipment in operation during the battery charging process requires a higher level of safety
- (2) The second solution considers the battery charging done inside of special stations built with this purpose in mind, followed by the battery distribution to integrated stations in need. This solution has some advantages and drawbacks, such as:
 - (2a) requires a distribution system
 - (2b) both special and integrated stations require a larger battery depositing space, a fact which results in improperly low utilization of space
 - (2c) the delay of battery replacement requires more batteries available for exchange to satisfy EVs necessities.

4 Case Study: Modelling Individual and Compounded V2G

This section contains a study regarding the integration of the EVs into the SGPS, addressing the processes of PEV battery charging and discharging.

4.1 Battery Charging Modelling

In the model representing the charging process, the location of the battery is always at the output of the power electronic converter which operates as a rectifier [11, 31]. The battery described by an equivalent capacitor C (see Fig. 4) represents a fair alternative regarding the analysis of the charging and discharging processes.

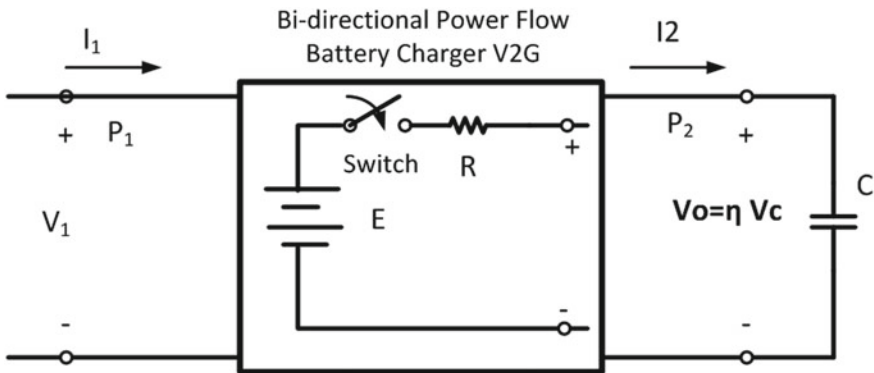


Fig. 4 Bi-directional power flow battery charger (V2G): equivalent circuit

However, the charging circuit is not a 100% efficient one, fact which explains the presence of a resistor R that characterizes the losses accounted for the charger. The rectifier, being the intermediate circuit between the charger's power supply and its output is stiff enough to provide a constant DC (rectified voltage) $V_{\text{int},rec}$ voltage. The switch meant to close the battery charging circuit turns on at the instant t_1 , triggering the appearance of the charging current $i_1(t)$.

$$V_{\text{int},rec} = V_R(t) + V_{\text{out}}(t) \quad (6a)$$

$$V_{\text{int},rec} = Ri_1(t) + \eta_C V_{\text{Cap}}(t) = \eta_C \frac{1}{C} \int_{t_1}^t i_2(\tau) d\tau \quad (6b)$$

The definition of the charger's efficiency in per-unit involves the ratio between the charger's output power to its input one (7).

$$\eta_C = \frac{P_{\text{out}}}{P_{\text{in}}} = \frac{V_{\text{out}}i_{\text{out}}}{V_{\text{in}}i_{\text{in}}} \quad (7)$$

One can express the Eq. (6b) in terms of currents following a time derivation, with the charging time constant $T_C = RC$:

$$R \frac{di_2(t)}{dt} + \frac{\eta_C}{C} i_2(t) = \frac{dV_{\text{int},rec}}{dt} = 0 \Rightarrow \frac{T_C}{\eta_C} \frac{di_2(t)}{dt} + i_2(t) = 0 \quad (8)$$

The solution for differential equation (8) comes the easiest whereas performing an intermediate Laplace conversion:

$$\frac{T_C}{\eta_C} [sI_2(s) - I_2(0)] + I_2(s) = 0 \Rightarrow I_2(s) = \frac{\frac{T_C}{\eta_C} I_2(0)}{\left(s + \frac{T_C}{\eta_C}\right)} \quad (9)$$

The initial value of the charging current is equal to $I_2(0) = V_{\text{int},rec}/R$, fact which leads to the current [31]:

$$i_2(t) = \frac{V_{\text{int},rec}}{R} \exp(-\eta_C t/T_C) \quad (10)$$

Introducing (10) into (6a and 6b), one can express the instantaneous voltage across the battery, considering the battery voltage at the beginning of the charging process being equal to $V_{\text{out}}(t_1)$:

$$v_{\text{out}}(t) = V_{\text{int},rec} [1 - \exp(-\eta_C t/T_C)] + V_{\text{out}}(t_1) \quad (11)$$

The battery status in terms of power requires the multiplication of each term of the Eq. (11) with the current expressed according to (10). It results the expression (12) which links the instantaneous power to the maximum power value and to the initial power as well.

$$\begin{aligned}
 P_{out}(t) &= \frac{V_{int,rec}^2}{R} [1 - \exp(-\eta_C t / T_C)] \exp(-\eta_C t / T_C) + \dots \\
 V_{out}(t_1) &= \frac{V_{int,rec}}{R} \exp(-\eta_C t / T_C)
 \end{aligned}
 \tag{12}$$

Whereas defining the maximum power at the battery as P_{max} (13a), respectively the initial power as $P(t_1)$ (13b) [11, 31]:

$$P_{max} = \frac{V_{int,rec}^2}{R} \exp(-\eta_C t / T_C)
 \tag{13a}$$

$$P(t_1) = V_{out}(t_1) \frac{V_{int,rec}}{R} \exp(-\eta_C t / T_C)
 \tag{13b}$$

One can express the instantaneous charging power as in (14).

$$P_{out}(t) = P_{max} [1 - \exp(-\eta_C t / T_C)] + P(t_1)
 \tag{14}$$

Considering the case of a PEV batteries during the charging process (power demand), the instantaneous power of the battery is [11, 31]:

$$P_{BPEV}(t) = P_{BPEV,max} [1 - \exp(-\alpha \eta_C t / T_{max})] + P(t_1)
 \tag{15}$$

The relation (16) presents the link between the efficiency of the charger η_C , charging constant of the battery α , charging time constant T_C , respectively the maximum time T_{max} . However, relation (15) lasts until the battery charging level reaches its fully charged required value $t_1 \leq t \leq t_{char}$. T_{max} represents the duration of battery to fully charge from zero power.

$$T_C = \left(\frac{\eta_C}{\alpha} \right) T_{max}
 \tag{16}$$

The initial PEV battery power level determines the duration of the charging process, if the battery reaches its prescribed maximum power value. In such a way, one can find the duration necessary for full charging as (17):

$$t_{char} = \begin{cases} 0 & P(t_1) = P_{BPEV,max} \\ T & P(t_1) = 0 \\ t_{char} & 0 < P(t_1) < P_{BPEV,max} \end{cases}
 \tag{17}$$

Combining the relations (15)–(17) and imposing $P_{BEV}(t_{char}) = P_{BEV,max}$, one can express the charging time as following (18):

$$\begin{aligned}
 P_{BPEV}(t_{char}) &= P_{BPEV,max} \\
 P_{BPEV,max} &= P_{BPEV,max} [1 - \exp(-\alpha\eta_C t_{char}/T_{max})] + P(t_1) \\
 P_{BPEV,max} \exp(-\alpha\eta_C t_{char}/T_{max}) &= P(t_1) \\
 \alpha\eta_C t_{char}/T_{max} &= -\ln\left(\frac{P(t_1)}{P_{BPEV,max}}\right) \Rightarrow t_{char} = -\frac{T_{max}}{\alpha\eta_C} \ln\left(\frac{P(t_1)}{P_{BPEV,max}}\right)
 \end{aligned}
 \tag{18}$$

The PEV power battery level, expressed for all the conditions is (19):

$$P_{BPEV}(t) = \begin{cases} P_{BPEV,max} [1 - \exp(-\alpha\eta_C t/T_{max})] + P(t_1) & t_1 < t < t_{char} \\ P_{BPEV,max} & t \geq t_{char} \end{cases}
 \tag{19}$$

One can estimate the total power demanded by the PEV battery for a full charge, starting from its initial status $P(t_1)$ as (20):

$$P_{BPEV,dem}(t) = P_{BPEV,max} - P_{BPEV}(t)
 \tag{20}$$

The expression (20) detailed for the full charging interval becomes (21a, 21b):

$$P_{BPEV,dem}(t) = P_{BPEV,max} - P_{BPEV,max} \exp(-\alpha\eta_C t/T_{max}), t_1 < t < t_{char}
 \tag{21a}$$

$$P_{BPEV,dem}(t) = 0, t \geq t_{char}
 \tag{21b}$$

Several scenarios in place lead to the evaluation of the battery charging in normal conditions and/or in presence of faults. For instance, if the PEV battery charging started at t_j is scheduled for a duration Δt_1 until the full charging completion, usually measured in hours [11]. A fault occurrence may stop the charging process prior to the full battery charge, let's say after an interval Δt_2 . The battery power level in such a case is (22):

$$P_{BPEV,dem}(t_1 + \Delta t_2) = P_{BPEV,max} \exp(-\alpha\eta_C \Delta t_2/T_{max}) - P(t_1), \Delta t_2 < \Delta t_1
 \tag{22}$$

If the fault occurs after the time scheduled for the PEV battery to reach its maximum charging level, then:

$$P_{BPEV,dem}(t_1 + \Delta t_2) = P_{BPEV,max}, \Delta t_2 > \Delta t_1
 \tag{23}$$

Whereas the fault is restored at the time $t_1 + \Delta t_3$, assuming no battery discharge during the time of fault occurrence and the time of operation restoration, one can assume a new initial power status for the battery power level (24):

$$P_{BPEV,dem}(t_1 + \Delta t_3) = P_{BPEV,max}(t_1 + \Delta t_2), \Delta t_3 > \Delta t_2 \quad (24)$$

Finally, the maximum battery power level appears after $t_1 + \Delta t_3 + \Delta t_1 - \Delta t_2$. One can calculate the overall energy required for the vehicle battery to fully charge, whereas the charger is unavailable because of a fault which lasts a certain time $\delta T_{Fault} = \Delta t_3 - \Delta t_2$ in terms of power and time (25).

$$E_{BPEV} = \begin{cases} \int_{t_1}^{t_1+\Delta t_2} P_{BPEV,dem}(\tau) d\tau & \Delta t_2 < \Delta t_1, t_1 < \tau < t_1 + \Delta t_2 \\ 0 & t_1 + \Delta t_2 < \tau < t_1 + \Delta t_3 \\ \int_{t_1+\Delta t_3}^{t_1+\Delta t_3+\Delta t_1-\Delta t_2} P_{BPEV,dem}(\tau) d\tau & t_1 + \Delta t_3 < \tau < t_1 + \Delta t_3 + \Delta t_1 - \Delta t_2 \end{cases} \quad (25)$$

In a parking lot with identical chargers (i.e., the same efficiency for each charger), whereas assuming the same level of maximum power, yet different charging rates α_i and different charging durations t_{chari} , one can express the total instantaneous power demand as [31] as a function of the total number of the PEVs.

$$P_{BPEV,dem}(t) = n_{PEV,C} P_{BPEV,max} - P_{BPEV,max} \sum_{i=1}^{n_{PEV,C}} \exp(-\alpha_i \eta_C t_{chari} / T_{max}) \quad (26)$$

4.2 Vehicle to Grid Modelling

The battery of a single PEV connected to the SGPS delivers power into the grid through the power electronic converter which operates in the inverter mode, with an efficiency η_{inv} . The battery discharge rate is γ_{dis} . If the process of power delivery into the grid starts at t'_1 , with the initial battery power level $P(t'_1)$, then the power discharging level at an instant t' is equal to:

$$P_{BPEV,dis}(t') = P(t'_1) \exp(-\gamma_{dis} \eta_i t' / T_{max}) - P_{BPEV,Lim} \quad (27)$$

The power limit level $P_{BPEV,Lim}$ represents the PEV battery power threshold necessary for starting the PEV engine, or driving it in electrical mode. In the latest situation, the battery cannot start the engine, yet the charger must do it, whereas the battery

must sustain the EV driving [31]. The power injected into the grid is equal to:

$$P_{BPEV,inj}(t') = P(t'_1) - P_{BPEV,dis}(t') \quad (28)$$

Consequently, introducing (28) into (27), one can express the power injected by the battery of a single PEV into the grid as (29).

$$P_{BPEV,inj}(t') = P(t'_1) \left[1 - \exp\left(-\gamma_{dis}\eta_i t' / T_{max}\right) \right] \quad (29)$$

The duration of the power injection into the grid strongly depends on the battery discharging constant γ_{dis} as well as the limit power P_{Lim} . At the end of the allowed discharging time t'_{dis} , the PEV battery discharging level is equal to zero.

$$P_{BPEV,dis}(t'_{dis'}) = 0 = P(t'_1) \exp\left(-\gamma_{dis}\eta_i t'_{dis'} / T_{max}\right) - P_{BPEV,Lim} \Rightarrow$$

$$t'_{dis} = -\frac{T_{max}}{\gamma_{dis}} \ln\left[\frac{P_{BPEV,Lim}}{P(t'_1)}\right], P_{BPEV,Lim} \leq P(t'_1) \quad (30)$$

If the power is injected into the grid for a duration equal to $\Delta t'$, in complete fulfillment of condition (27), then the energy impressed into the grid is:

$$E_{BPEV,inj} = \int_{t'}^{t'+\Delta t'} P(t') \left[1 - \exp\left(-\gamma_{dis}\eta_i t' / T_{max}\right) \right] dt; t' \leq t'_{dis} \quad (31)$$

If instead of one PEV there are n_{PEV} PEVs, injecting power to the grid for the durations $t_{sup,k}$, having the discharging constants of the batteries $\gamma_{dis,k}$ and the initial powers $P_k(t'_1)$, one can evaluate the total power impressed into the grid at the instant t' as (32):

$$P_{BPEV,inj}(t') = \sum_{k=1}^{n_{PEV,D}} P_k(t'_1) \left[1 - \exp\left(-\gamma_{dis,k}\eta_i t_{sup,k} / T_{max}\right) \right] \quad (32)$$

However, the presence of the overall V2G interaction has a dynamic character, there are PEV with batteries under charging, vehicles which retrieve energy into the SGPS, and their number is in continuous change. The authors of [31] assembled a model of a sized parking lot, suitable for estimating the net value of the power submitted or received from the SGPS, as well as the net energy impressed to the SGPS, whereas the vehicles are parked and connected. Using probabilistic calculations, the modeling study continues with the inclusion of the influx, respectively outgoing vehicles, the service duration allocated to vehicles, and the approximation of the battery initial charging level. The approach to the PEV diversity relies on the

differences in charging and discharging coefficients. Finally, the addition of some renewables to the PEV parking lot offer a more complete picture.

4.3 Modelling of the EV Parking Lot Operation

The resultant (net) power exchange between the PEV fleet and the grid (33) represents the difference between the injected power and the power demanded by the vehicles for charging (26), (32):

$$P_{BPEV,net} = \sum_{k=1}^{n_{PEV,D}} P_k(t'_1) [1 - \exp(-\gamma_{dis,k} \eta_i t_{sup,k} / T_{max})] - P_{BPEV,max} \left[n_{PEV,C} - \sum_{i=1}^{n_{PEV,C}} \exp(-\alpha_i \eta_C t_{chari} / T_{max}) \right] \quad (33)$$

The net energy injection into the grid results from the integration of (33) over a certain amount of time of interest. Moreover, imposing the non-existence of charging over a 24 h time span, one can estimate the energy retrieved into a storage facility and obtain important data to design such a facility [31]. Such an energy expression displays the form:

$$E_{BPEV,net} = \sum_{k=1}^{n_{PEV,D}} P_k(t'_1) \left\{ t_{sup,k} - \frac{T_{max}}{\eta_i t_{sup,k}} [1 - \exp(-\gamma_{dis,k} \eta_i t_{sup,k} / T_{max})] \right\} - P_{BPEV,max} \frac{T_{max}}{\eta_C} \sum_{i=1}^{n_{PEV,C}} \left\{ \frac{\eta_C t_{chari}}{T_{max}} - \frac{[1 - \exp(-\alpha_i \eta_C t_{chari} / T_{max})]}{\alpha_i} \right\} \quad (34)$$

The power, respectively the energy gain factors are defined by dividing the power, respectively the energy inserted into the supply, respectively by the product of the number of charging stations to the maximum power of a station.

$$G_{Power} = \frac{\sum_{k=1}^{n_{PEV,D}} P_k(t'_1) [1 - \exp(-\gamma_{dis,k} \eta_i t_{sup,k} / T_{max})]}{N_{st} P_{max}} \quad (35)$$

$$G_{En} = \frac{\sum_{k=1}^{n_{PEV,D}} P_k(t'_1) \left\{ t_{sup,k} - \frac{T_{max}}{\eta_i t_{sup,k}} [1 - \exp(-\gamma_{dis,k} \eta_i t_{sup,k} / T_{max})] \right\}}{N_{st} P_{max}} \quad (36)$$

The renewable energy presence generally comes through arrays of photovoltaic panels (PV), wind farms. However, due to the irregularities in energy delivery recorded by renewables, the aggregators strongly recommend the access to a power

system containing stable power sources from thermal and nuclear power plants, hydroelectric plants and so on. In presence of renewables the net power is (37).

$$P_{BPEV,net} = \sum_{k=1}^{n_{PEV,D}} P_k(t'_1) [1 - \exp(-\gamma_{dis,k} \eta_i t_{sup,k} / T_{max})] - P_{BPEV,max} \left[n_{PEV,C} - \sum_{i=1}^{n_{PEV,C}} \exp(-\alpha_i \eta_C t_{chari} / T_{max}) \right] + P_{renewables} \tag{37}$$

5 Case Study: Simulations, Results and Discussion

In the case of individual vehicles, simulations targeted the battery power status of two different plug in electric vehicles during the power demand (charging), respectively power supply to the grid (discharging). The hypothetical PEVs under scrutiny have the characteristics of interest displayed in Table 4.

This assessment procedure applied to the PEVs battery charging and discharging processes relies on a methodology derived from the one proposed in [31] and continued in [11]. At the first step of simulations, one subjected the batteries of both PEVs to a full charge from 0 to 100% power. The charge efficiency values (i.e., operating in this case as rectifier), are: 50, 70, 90% and the ideal of 100%. The advantage of a faster charging process at high efficiency comes with the drawback of increased power demand from the supply, according to Fig. 5. For the same efficiency value, the battery charging performance, according to (15) and (19) is an intrinsic characteristic of an individual PEV.

In a similar manner, simulations regarding the PEV battery discharging during the time allocated for energy supply to the grid, regards the higher converter efficiency (i.e., inverter operation of the charger) due a faster discharge process (see Figs. 6 and 7), according to (29), which means a faster response to the grid demand. Although, faster charging/discharging processes, even benefiting the PEV operation, respectively the grid may result in severe shortening of the battery lifespan.

Table 4 Characteristics of plug-in electrical vehicles under study

Characteristic	PEV1	PEV2
Battery power at full charge (kW)	150	75
Maximum charge duration T_{max} (h)	4	8
Charging coefficient α_{C1}	9.75	8.25
Charging coefficient α_{C2}	6.75	4.75
Discharging coefficient γ_{dis1}	10.15	8.75
Discharging coefficient γ_{dis2}	5.00	4.0

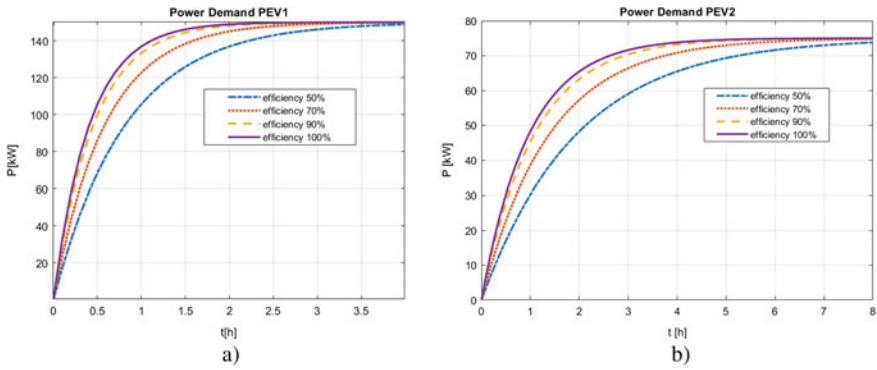


Fig. 5 Time dependency of the power demand for PEV1 (a) and PEV2 (b) influenced by the battery charger efficiency

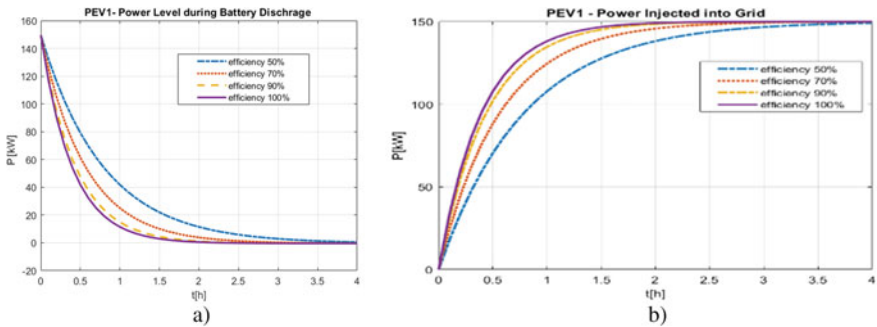


Fig. 6 Time dependency of the power discharge (a) and power injected into the grid (b) for PEV1 influenced by the inverter efficiency

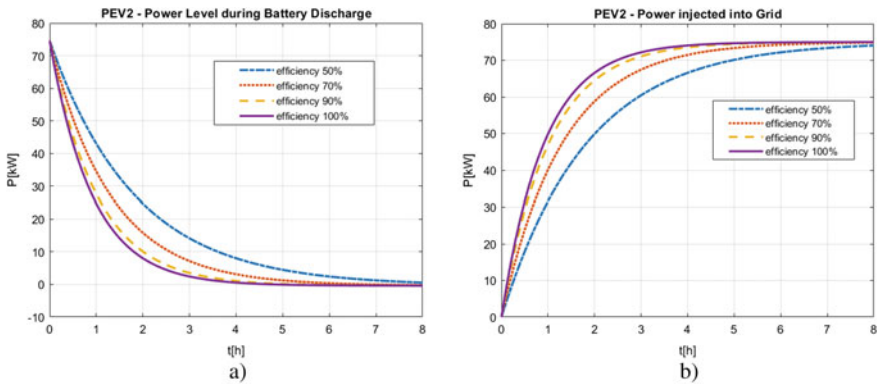


Fig. 7 Time dependency of the power discharge (a) and power injected into the grid (b) for PEV2 influenced by the inverter efficiency percent value

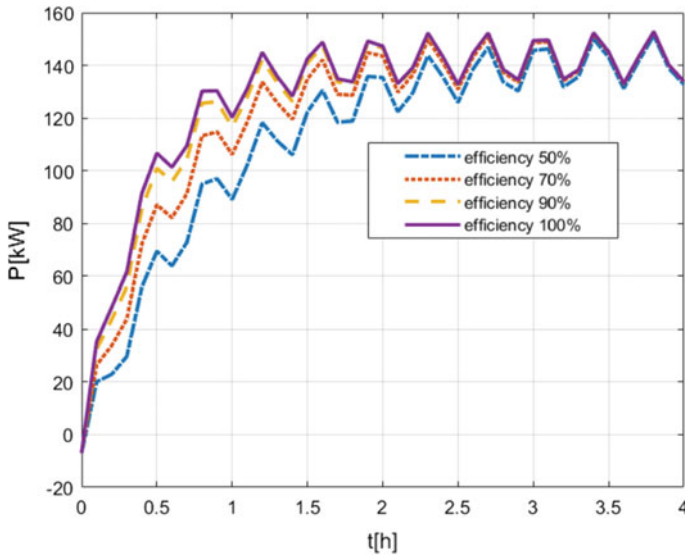


Fig. 8 Time dependency of the power demand for PEV1 in presence of renewable energy sources, for a battery charging coefficient $\alpha_C = 9.75$

Considering the presence of the renewable energy sources, the power demand, reflected at the level of individual PEVs appears in Figs. 8, 9, 10 and 11. A time alternating function of approximately 2 cycles per hour mimics the presence of wind generators. In such a scenario, the SGPS doesn't have a connection to storage units like stationary battery arrays or main power system which includes classical (i.e. fossil fuel based) energy sources. The presence of renewables leads to approximate power ripples of 15% for PEV1, respectively 30% for PEV2. One can observe the fact that charging coefficients play a role as well: the higher value of the charging coefficient, the faster the process is (Figs. 9 and 10).

Taming the intermittency and randomness from the existing power-time profile of renewables (see Figs. 12 and 13), requires the presence of fast compensation function at the point of common coupling between the PEV, SGPs, stationary power storage batteries and eventually main power supply.

In a similar assumption of present renewable energy sources, the PEVs deliver power to the grid, having a profile, reflected at the level of individual PEVs appearing in Figs. 14, 15, 16 and 17. Renewable sources are identical to the ones present in the simulations regarding individual battery charging. The presence of renewables leads to approximate power ripples of 15% for PEV1, respectively 30% for PEV2, as well. One can observe the fact that discharging coefficients play a role as well: the higher value of the discharging coefficient, the faster the process is (Figs. 14 and 16).

Charging process regarding a parking lot requires scenarios in which the involvement of multiple vehicles requires certain assumptions made regarding the initial level of battery charging, respectively the durations necessary to reach certain levels

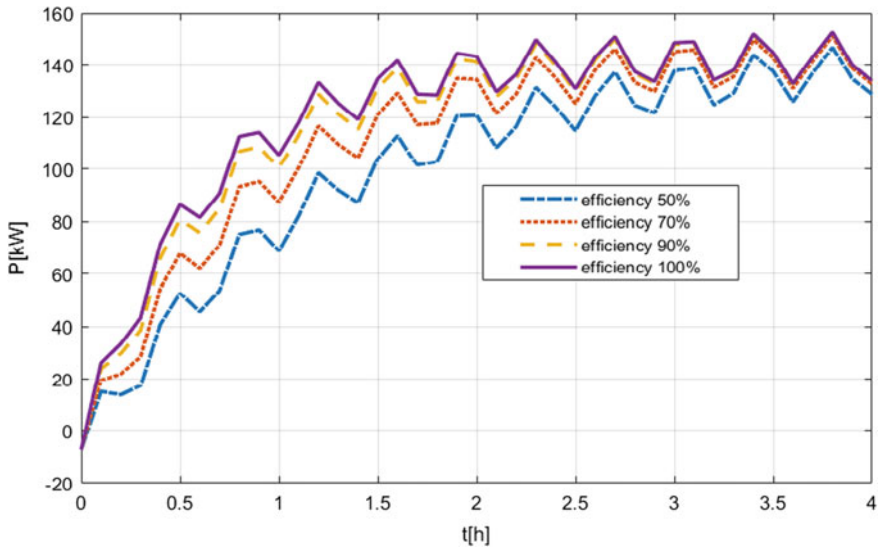


Fig. 9 Time dependency of the power demand for PEV1 in presence of renewable energy sources, for a battery charging coefficient $\alpha_C = 6.75$

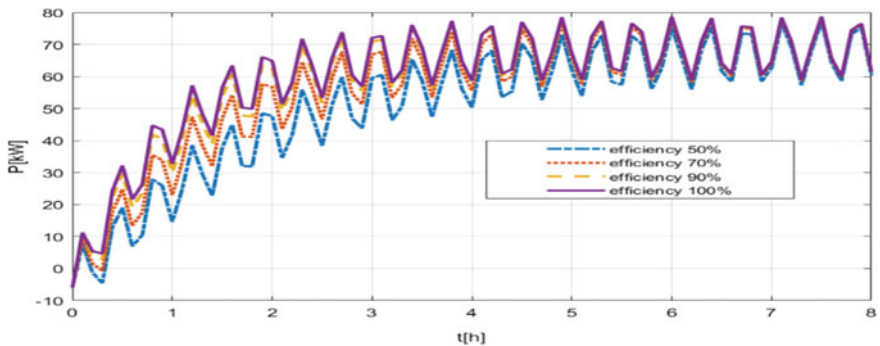


Fig. 10 Time dependency of the power demand for PEV2 in presence of renewable energy sources, for a battery charging coefficient $\alpha_C = 8.25$

of battery charging. For the multiple vehicles charging scenario, we've assumed the presence of 30 PEVs: 15 PEV1s and 15PEV2s. The efficiency of the charger, operating as rectifier is 95%, whereas the upper limit of the battery power charging is 90% of the maximum power for both types of PEVs using Level 2 chargers:

- 5 PEV1s at 0% initial power level before starting charging, 6 PEV1s at 20% initial power level, respectively 4 at 40% power level.
- 8 PEV2s at 0% initial power level before starting charging, 5 PEV1s at 30% initial power level, respectively 2 at 50% power level.

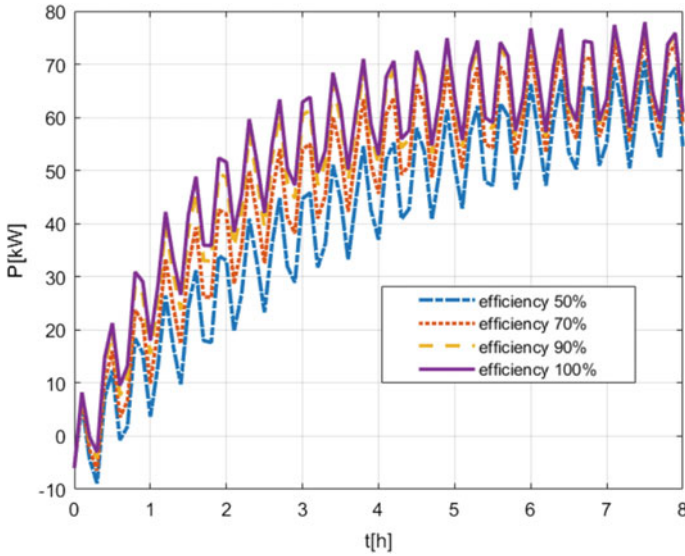


Fig. 11 Time dependency of the power demand for PEV2 in presence of renewable energy sources, for a battery charging coefficient $\alpha_C = 4.75$

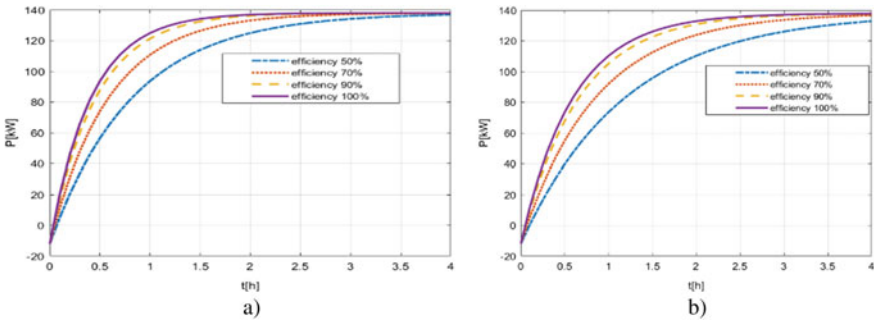


Fig. 12 Time dependency of the power demand for PEV1 in presence of compensated renewable energy sources, for a battery charging efficiency $\alpha_C = 9.75$ (a), respectively $\alpha_C = 6.75$ (b)

- For PEV1 is necessary 3/4 of the maximum charging time to reach 90% level from 0% initial power level, 1/2 of the maximum charging time to reach 90% level from 20% initial power level, respectively 1/4 of the maximum charging time to reach 90% level from 40% initial power level.
- For PEV2 is necessary 4/5 of the maximum charging time to reach 90% level from 0% initial power level, 1/2 of the maximum charging time to reach 90% level from 30% initial power level, respectively 1/4 of the maximum charging time to reach 90% level from 50% initial power level.
- The maximum charging durations of PEV1 and PEV2 appear in Table 4.

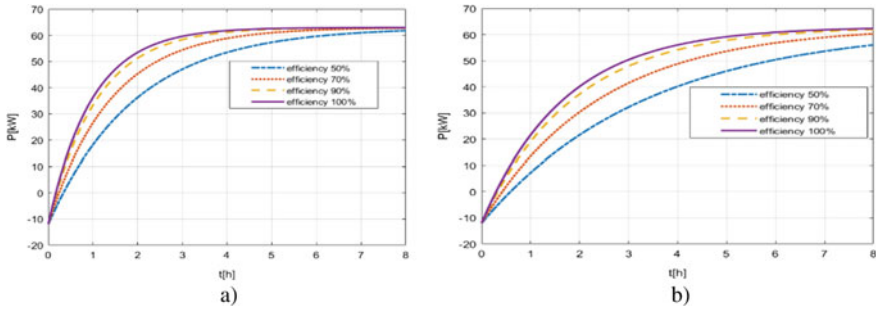


Fig. 13 Time dependency of the power demand for PEV2 in presence of renewable energy sources, for a battery charging efficiency $\alpha_C = 8.25$ (a), respectively $\alpha_C = 4.75$ (b)

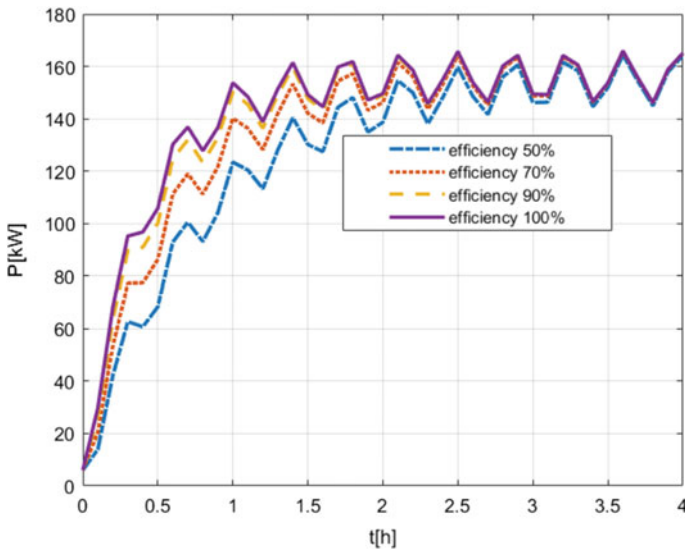


Fig. 14 Time dependency of the power injected into the grid from PEV1 in presence of renewable energy sources, for a battery discharging coefficient $\gamma_{dis} = 10.15$

- The application of (26) in the circumstances from above resulted in the following values of the charging coefficients: for PEV1 $\alpha_{C1, PEV1} = 3.2317$, $\alpha_{C2, PEV1} = 2.5347$, $\alpha_{C3, PEV1} = 3.29185$, $\alpha_{C1, PEV2} = 3.0297$, $\alpha_{C1, PEV2} = 1.929$, $\alpha_{C1, PEV1} = 2.1508$.

Following simulations involving charging the batteries of multiple vehicles from the same parking lot, without (see Fig. 18) and in presence of renewables (see Fig. 19), one can extract the power–time profile for charging, with a variation within 8 MW during the considered duration. Multiple scenarios can result in significant data, suitable for interpretation, stochastic calculations and finally in optimization functions.

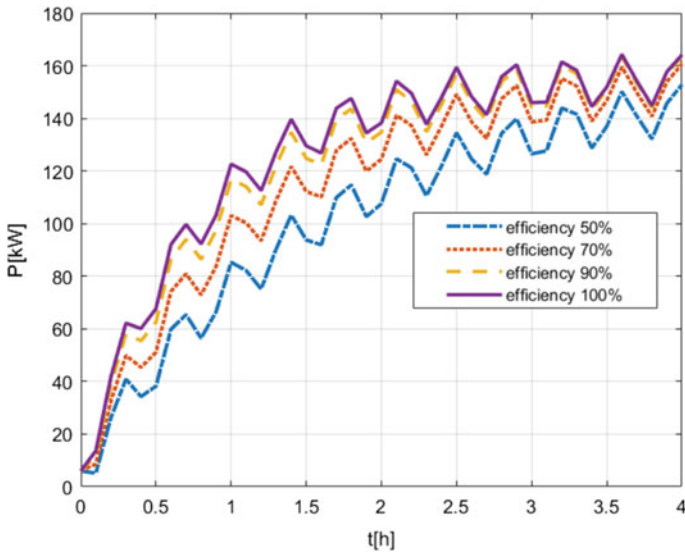
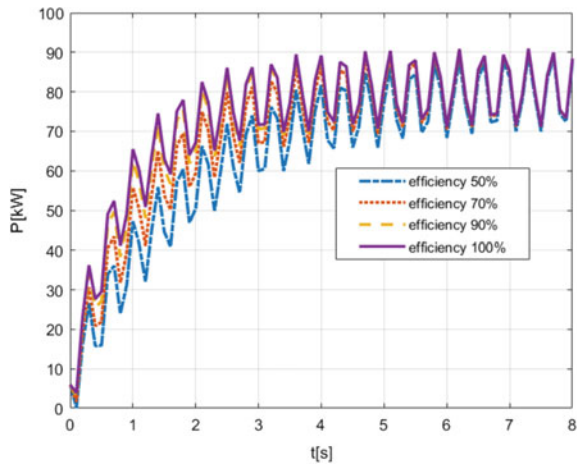


Fig. 15 Time dependency of the power injected into the grid from PEV1 in presence of renewable energy sources, for a battery charging coefficient $\gamma_{dis} = 5.0$

Fig. 16 Time dependency of the power injected into the grid from PEV2 in presence of renewable energy sources, for a battery charging coefficient $\gamma_{dis} = 8.75$



Although most of optimization functions cover domains like driving scheduling, emissions mitigation and revenues/taxes, the input from PEVs battery charging process characteristics, the interaction with SGPS, with and/or without compensated renewables proven very useful when commissioning elements of SGPS.

Power supply to the grid from a compound of vehicles from a parking lot, during the V2G operation, relies on discharging the batteries of these vehicles. Discharging process is faster than charging one [11], whereas the discharging process must

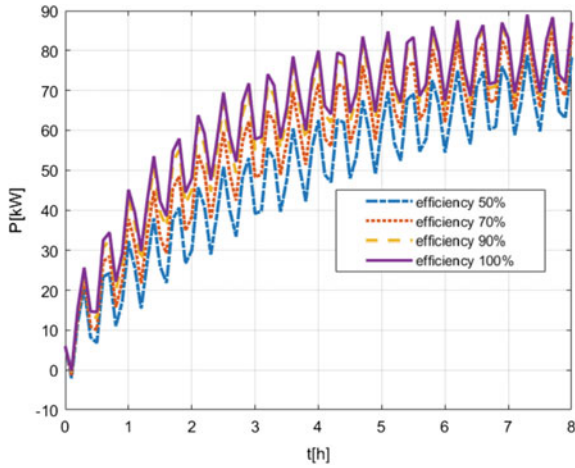


Fig. 17 Time dependency of the power injected into the grid from PEV2 in presence of renewable energy sources, for a battery charging coefficient $\gamma_{dis} = 4.0$

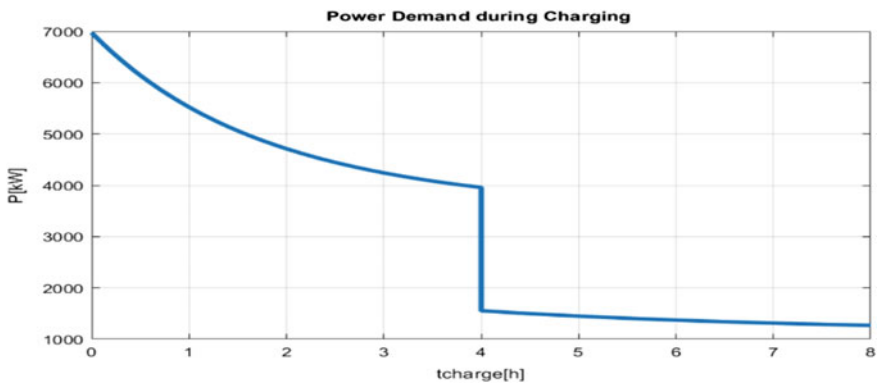


Fig. 18 Time dependency of the power demanded from the grid by the compounded PEV1 and PEV2 consumers from the parking lot, without involving renewable energy

encounter the low power threshold limit. Such a limit largely varies with respect to the type of vehicle and the next outcome of the PEV after providing energy to the SGPS during the power demand intervals (i.e., whether would live the parking lot for a drive or will stay for charging when available and for how long, and so for).

In this simulation regarding the battery discharging there were considered 10 PEV1s and 10 PEV2s, retrieving energy into SGPS through the same Level 2 chargers working as inverters.

- All 10 PEV1s and all 10PEV2s are fully charged when starting to supply the SGPS.

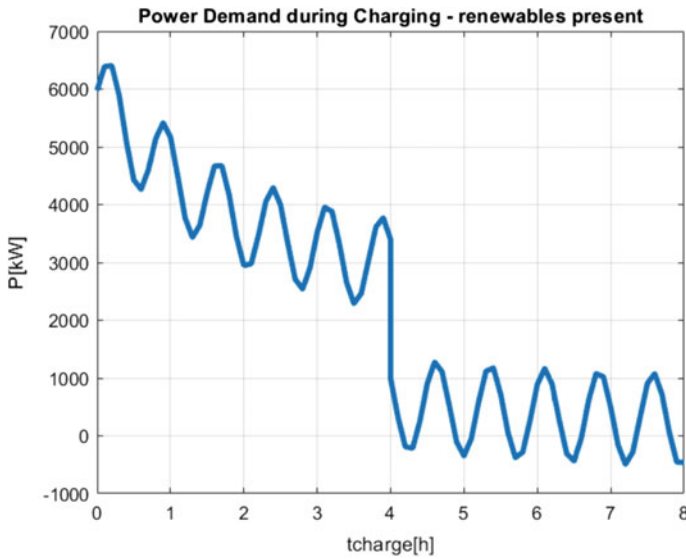


Fig. 19 Time dependency of the power demanded from the grid by the compounded PEV1 and PEV2 consumers from the parking lot, involving the presence of the fluctuating renewable energy sources

- The power level of the PEV1s battery drops from 100 to 5% (95% discharge) in 1/3 of its maximum charging time (see Table 4).
- The power level of the PEV2s battery drops from 100 to 10% (90% discharge) in 1/4 of its maximum charging time (see Table 4).
- The low power limit of the PEV1s is 4 kW, whereas for PEV2s is 2 kW.
- The application of (29) in the frame of the assumptions from above, results into the following discharging coefficients: $\gamma_{\text{dis,PEV1}} = 8.11$, respectively $\gamma_{\text{dis,PEV2}} = 8.70$.
- Because the battery discharging process is much faster than the charging one, we've considered four identical batches of vehicles performing V2G for a total duration equal to the maximum charging time of PEV2.

For this case of simulation, the intrinsic variability of the nature of the V2G model (Fig. 20) covers about 2 MW and has a cyclical nature. In a parking lot of vehicles demanding power and those who supply the SGPS coexist. To simulate such a regime, one superimposed the previous two scenarios, charging and discharging. The battery discharging is much faster, fact that explains the power-time profile is modulated by the profile of power demand, whereas presents a ripple following the cyclical character of the power-time profile recorded for V2G operation. Following the alternative character of the renewables of “wind generation” type, one can obtain a net power-time profile in presence of renewables (37), according to Fig. 21, or after compensating the renewables intermittency (33), according to Fig. 22.

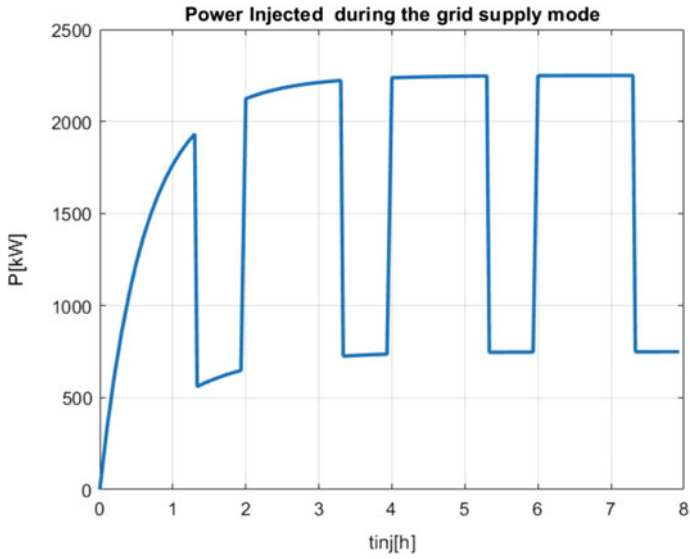


Fig. 20 Time dependency of the power injected into the grid by the compounded PEV1 and PEV2 suppliers from the parking lot, without involving renewable energy

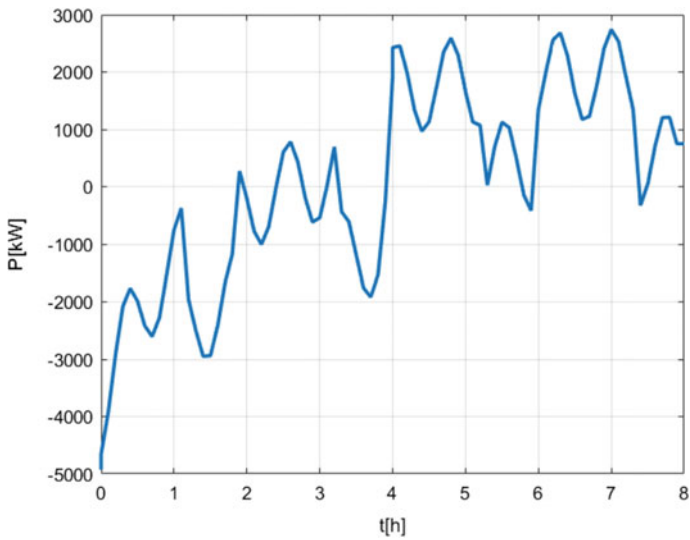


Fig. 21 Time dependency of the net power exchanged with the grid by the compounded PEV1 and PEV2 suppliers from the parking lot, involving the presence of fluctuating renewable energy

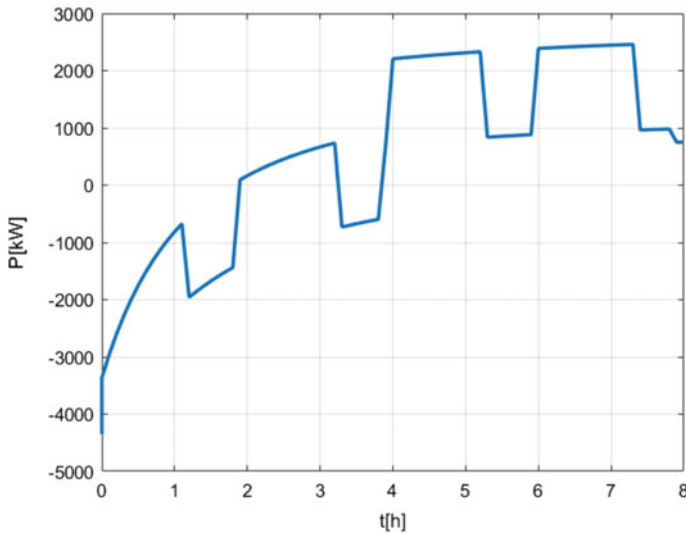


Fig. 22 Time dependency of the net power exchanged with the grid by the compounded PEV1 and PEV2 suppliers from the parking lot, involving the presence of compensated renewable energy

Although is highly unlikely to have a positive net power for long durations, the impact of the PEVs operation in V2G is beneficial for diminishing the overall energy consumption. The gain factors (35) and (36) became objective functions which can lead to optimization of parking lot power flow as function of time and provide information as input for two directions: the PEVs traffic schedules and revenue increase. Each of this direction operates in terms of own family of optimization functions, which can be minimized/maximized for optimal results [31].

Another study involves a system in a configuration similar the one from Fig. 1. The example originates from an application presented on the *MATLAB/Simulink portal* [32], treating a V2G system performing one of its ancillary duties: frequency regulation on a relatively small SGPS. All the SGPS components operate at a three-phase power supply rated for 25 kV. The connection to the SGPS for both, the wind farm and the photovoltaic required the presence of a standard step-up transformer following the output inverters, considered sinusoidal. There is no reference to harmonics in this section. A step-down transformer brings the voltage level to the EV, respectively, residential consumers. For simplification reasons, one can ignore the necessity of another intermediate step-down transformer to the residential consumers. The V2G participants are:

- (a) One fossil-fuel-based (Diesel) generator with the nameplate data: $S_n = 30 \text{ MW}$, $V_n = 25 \text{ kV}$, $f_n = 60 \text{ Hz}$, driven by a 30 MW Diesel Engine
- (b) One Wind Farm rated for: $SWF = 6 \text{ MW}$, nominal wind speed 12.5 m/s, maximum wind speed 15 m/s

- (c) One Photovoltaic Farm rated for $SPV = 9\text{ MW}$, efficiency 11%, radiant surface $70,000\text{ m}^2$
- (d) Three Phase transformer rated for $S_T = 50\text{ MVA}$, $V_1/V_2 = 25/0.46\text{ kV}$
- (e) The community has 1200 homes, with a ratio of 1:10 eV owners/(total households). The load contains a residential type of consumers as well as a low power induction machine, has a consumption profile and a given power factor. The induction machine, as the largest single consumer has the following data:
 $P_n = 200\text{ kW}$, $V_n = 600\text{ V}$, $f_n = 6\text{ Hz}$, $R_S = 0.0278\text{ pu}$, $X_{IS} (L_{IS}) = 0.1091\text{ pu}$,
 $X_m (L_m) = 2.974\text{ pu}$, $R_r = 0.0328\text{ pu}$, $X_{lr} (L_{lr}) = 0.1997\text{ pu}$.
- (f) 120 New EVs, with a nominal power $PEV = 150\text{ kW}$ each, and a charger efficiency of 95%.

The EVs operate under the V2G technology, and their batteries are in the charging mode when the power from SGPS is in excess, respectively in discharging mode when there is a deficit of power from SGPS. The interval under study comprised a full 24 h interval, whereas the profiles proposed in [32] by MathWorks and adopted here include all possible states for an EV. The profiles are:

- Profile #1(42 cars): Going to work and charge the battery car there
- Profile #2(25 cars): Going to work and charge the battery car after a more extended trip
- Profile #3(15 cars): Going to work and charge the battery car after the arrival at home
- Profile #4(25 cars): Stay at home
- Profile #5(12 cars): Working night shift

The simulation covers 24 h. The solar radiance follows a normal distribution function with the maximum in the middle of the day, with partial shading at noon, whereas the wind has a very irregular profile, respectively one trip due to excessive speed at 10.00 pm. After running the simulation, the power distribution functions appear in Figs. 5, 6, 7 and 8. The shape of power indicates the effectiveness of the voltage regulation process (Figs. 23, 24 and 25).

The renewable energy sources have a cumulated installed power of 15 MW, equal to 50% of the nominal power of the diesel generator. The total power of the PEVs is

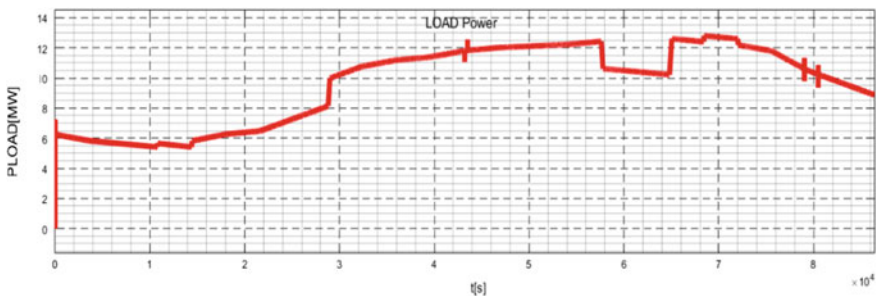


Fig. 23 Real Power at the load during an interval of 24 h (expressed in seconds)

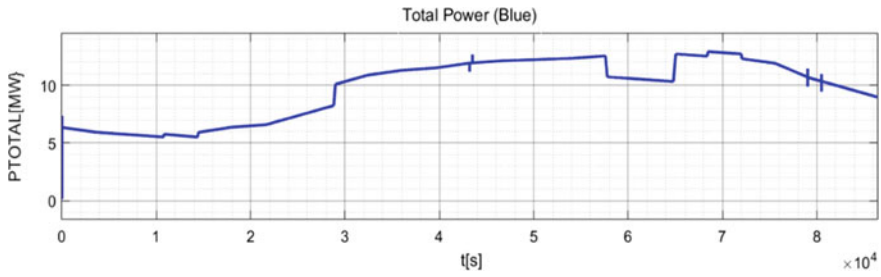


Fig. 24 Total Real Power during an interval of 24 h (expressed in seconds)

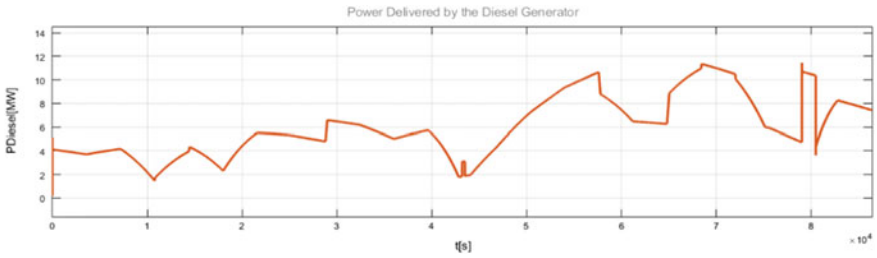


Fig. 25 Total real power delivered by the diesel generator during an interval of 24 h (expressed in seconds)

equal to 18 MW. However, the renewable energy harvested from both solar panels and wind generators is intermittent (see Fig. 26), whereas the nature of interaction between the PEVs and SGPS follows the profiles 1 through 5. All the consumers and generators determine a load power–time profile presented in (24), with all groups having an important participation to the total power, with respect to the principal power source, the Diesel generator.

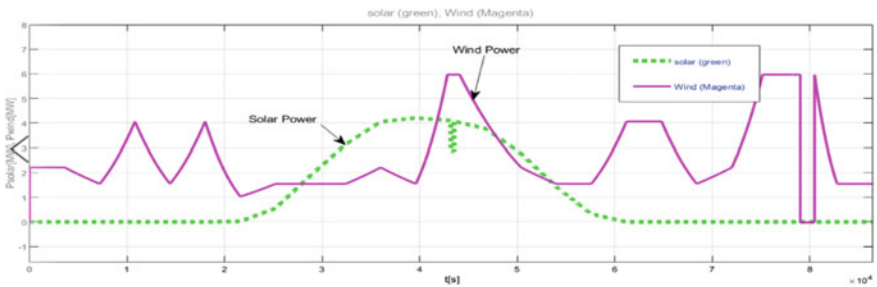


Fig. 26 Total real power delivered by the solar panels array and wind generators during an interval of 24 h (expressed in seconds)

6 Conclusion

The EVs, due to the V2G capability of bi-directional power transfer, can play the role of the consumer as one of the producers as well, capable of smoothening the power irregularities from wind and solar power sources. Besides the advantage of being the energy beneficiary, and the merit of being present when the SGPS needs, the EV battery plays the ancillary roles of power regulation, spinning reserves, and compensator for reactive power. Challenges faced by SGPS due to the presence of the power electronic converters involved in the EV charging/discharging process accompany the drawback of the life span shortening suffered by the EV batteries. The models presented in this chapter address the charging and discharging processes subjecting individual and multiple PEVs, through simulations, with and without the impact of the intermittent character of renewables. The primary outcome of the simulation regards the power–time profile in conditions of battery charging, supply to the grid, and mixed. The impact of the intermittent renewable sources reflects an increased power variability, indicating the need for compensation using stationary storage systems or accepting classical, fossil fuel-based energy sources at the point of common coupling. The latter are stable sources which smoothen the overall power–time profile. The net power determined through simulations becomes a candidate for “objective function” status, and its maximization becomes possible. The power or energy gain factors, derived from the net energy appear suitable as objective functions, and both include revenue elements. However, the construction procedure targeting all these objective functions must include stochastic algorithms for accuracy purposes. The last simulation, built-up derived from a MATLAB/Simulink existing application and could offer information about the electric power profile over 24 h and in different points of the integrated system. There are several treatments for the shortcomings regarding the EVs integration, and optimal scheduling for driving and charging are amongst them. However, the main reasons which make the V2G impractical for now are the reduced number of vehicles, unattractive compensation for the participating EV owners as well as the anxiety of losing the driving range whereas the EVs participate in V2G joint venture. However, many models indicated profitability for the distributor and aggregator. There are two distinct groups of standards following the subject of application: EV and SGPS, both addressing similar topics, yet from different referential.

References

1. Kempton W, Letendre SE (1997) Electric vehicles as power source for utilities. *Transp Res D* 2(3):157–175
2. Liu L, Kong F, Liu X, Peng Y, Wang Q (2015) A review on electric vehicles interacting with renewable energy in smart grid. *Renew Sustain Energy Rev* 51:648–661
3. Shaikat N, Khan B, Mehmood CA, Khan J, Farid U, Majid M, Anwar SM, Jawad M, Ullah Z (2018) A survey on electric vehicle transportation within smart grid system. *Renew Sustain Energy Rev* 81:1329–1349

4. Tan KM, Ramachandaramurthy VK, Yong JY (2016) Integration of electric vehicles in smart grid: a review on vehicle to grid technologies and optimization techniques. *Renew Sustain Energy Rev* 53:720–732
5. Francis Mwasilu F, Justo JJ, Kim EK, Do TD, Jung JW (2014) Electric vehicles and smart grid interaction: a review on vehicle to grid and renewable energy sources integration. *Renew Sustain Energy Rev* 34:501–516
6. Yang Z, Li K, Foley A, Zhang C (2014) Optimal scheduling methods to integrate plug-in electric vehicles with the power system: a review. Preprints of the 19th world congress the international federation of automatic control Cape Town, South Africa, August 24–29, 2014, pp 8595–8603
7. Xydias E, Marmaras C, Cipcigan Liana M, Jenkins N, Carroll S, Barker M (2016) A data-driven approach for characterising the charging demand of electric vehicles: a UK case study. *Appl Energy* 162:763–771
8. Green RC II, Wang L, Alam M (2011) The impact of plug-in hybrid electric vehicles on distribution networks: a review and outlook. *Renew Sustain Energy Rev* 15:544–553
9. Rezvani Z, Jansson J, Bodin J (2015) Advances in consumer electric vehicle adoption research: a review and research agenda. *Transp Res Part D* 34:122–136
10. Krupa JS, Rizzo Donna M, Eppstein Margaret J, Lanute BD, Gaalema Diann E, Lakkaraju K, Warrender Christina E (2014) Analysis of a consumer survey on plug-in hybrid electric vehicles. *Transp Res Part A* 64:14–31
11. Reddy GH, Goswami AK, Choudhury NBD (2018) Impact of plug-in electric vehicles and distributed generation on reliability of distribution systems. *Int J Eng Sci Technol* 21:50–59
12. Anastasiadis AG, Kondylis GP, Pilizakis A, Vokas G (2019) Effects of increased electric vehicles into a distribution network. *Energy Procedia* 157:586–593
13. Qian K, Zhou C, Yuan Y (2015) Impacts of high penetration level of fully electric vehicles charging loads on the thermal ageing of power transformers. *Electr Power Energy Syst* 65:102–112
14. Godina R, Rodrigues EMG, Paterakis NG, Erdinc Catalão JPS (2016) Impacts of high penetration level of fully electric vehicles charging loads on the thermal ageing of power transformers. *Energy Convers Manag* 120:206–216
15. Geske J, Schumann D (2018) Willing to participate in vehicle-to-grid (V2G)? Why not! *Energy Policy* 120:392–401
16. Rebecca Gough, Dickerson C, Rowley P, Walsh C (2017) 1 Vehicle-to-grid feasibility: a techno-economic analysis of EV-based energy storage. *Appl Energy* 92:12–23
17. Bhandari V, Sun K, Frances Homans (2018) The profitability of vehicle to grid for system participants—a case study from the Electricity Reliability Council of Texas. *Energy* 153:278–286
18. Darlene S (2017) Critical elements of vehicle-to-grid (V2G) economics. Strategic partnership project Report NREL/TP-5400-69017 September 2017. National Renewable Energy Laboratory 15013 Denver West Parkway Golden, CO 80401 303-275-3000. www.nrel.gov
19. Zakariazadeh A, Jadid S, Siano P (2015) Integrated operation of electric vehicles and renewable generation in a smart distribution system. *Energy Convers Manag* 89:99–110
20. Michela Longo, Federica Foadelli, Wahiba Yaïci (2019) Electric vehicles integrated with renewable energy sources for sustainable mobility book: new trends in electrical vehicle powertrains. *IntechOpen* 10:203–223
21. Fazelpour F, Vafaeipour M, Omid Rahbari O, Rosen MA (2014) Intelligent optimization to integrate a plug-in hybrid electric vehicle smart parking lot with renewable energy resources and enhance grid characteristics. *Energy Convers Manag* 77:250–261
22. Rahbari O, Vafaeipour M, Omar N, Marc A, Rosen MA, Hegazy O, Timmermans JM, Heibati S, Peter Van Den Bossche P (2017) An optimal versatile control approach for plug-in electric vehicles to integrate renewable energy sources and smart grids. *Energy* 134:1053–1067
23. Honarmand M, Zakariazadeh A, Shahram Jadid S (2014) Optimal scheduling of electric vehicles in an intelligent parking lot considering vehicle-to-grid concept and battery condition. *Energy* 65:572–579

24. Wang Z, Wang L, Dounis AI, Yanga R (2012) Integration of plug-in hybrid electric vehicles into energy and comfort management for smart building. *Energy Build* 47:260–266
25. Battistelli C, Baringo L, Conejo AJ (2012) Optimal energy management of small electric energy systems including V2G facilities and renewable energy sources. *Electr Power Syst Res* 92:50–59
26. Haddadian G, Khalili N, Khodayar M, Shahidehpour M (2016) Optimal coordination of variable renewable resources and electric vehicles as distributed storage for energy sustainability. *Sustain Energy Grids Netw* 6:14–24
27. Uddin K, Dubarry M, Glick MB (2018) The viability of vehicle-to-grid operations from a battery technology and policy perspective. *Energy Policy* 113:342–347
28. Peng C, Zou J, Lian L, Li L (2017) An optimal dispatching strategy for V2G aggregator participating in supplementary frequency regulation considering EV driving demand and aggregator's benefits. *Appl Energy* 190:591–599
29. Bishop JDK, Axon CJ, Bonilla D, Banister D (2016) Estimating the grid payments necessary to compensate additional costs to prospective electric vehicle owners who provide vehicle-to-grid ancillary services. *Energy* 94:715–727
30. Richardson DB (2013) Encouraging vehicle-to-grid (V2G) participation through premium tariff rates. *J Power Sources* 243:219–224
31. Chukwu UC, Mahajan SM (2014) V2G Parking lot with RV rooftop for capacity enhancement of a distribution system. *IEEE Trans Sustain Energy* 5(1):119–127
32. www.mathworks.com